Turbulence to turbulence transition in homeotropically aligned nematic liquid crystals

D. E. Lucchetta, N. Scaramuzza, G. Strangi, and C. Versace*
Dipartimento di Fisica dell'Università della Calabria and Istituto Nazionale per la Fisica della Materia, I-87036 Rende, Cosenza, Italy
(Received 22 January 1999)

In this paper, a study of the electrically driven turbulent-turbulent transition in a homeotropically oriented nematic sample is reported. The transition has the characteristics of a nucleation process, and its threshold has been experimentally determined. The nucleation rate and the growth velocity of the new turbulent nuclei are also reported. [S1063-651X(99)05807-9]

PACS number(s): 61.30.−v

INTRODUCTION

The transition between two different turbulent regimes is not a very common phenomenon in nature [1]. Among the best known systems are the turbulent-turbulent transition in superfluid helium [2] and the dynamic scattering mode1–dynamic scattering mode 2 (DSM1-DSM2) transition in nematic liquid crystals (NLC) under a planar anchoring condition [3]. Lately the transition between turbulent states driven by an external voltage has also been observed in a homeotropic aligned nematic liquid crystal sample [4].

In the last few years, electrodynamic instabilities in homeotropically oriented layers of negative dielectric anisotropy nematics have attracted the interest of a discrete number of authors [5–9]; in fact, although the homeotropic orientation shows a less rich scenario it differs dramatically from the planar case. The electroconvective rolls occur as a secondary instability after the Fréedericksz one [10]. Furthermore, because at the Fréedericksz transition the nematic director spontaneously chooses a bend direction, a spontaneous breaking of the isotropic symmetry occurs, which makes possible a direct transition to the spatial chaos [8,11].

From a strictly phenomenological point of view, when a low frequency electric voltage is applied to a homeotropic sample of NLC with a negative dielectric anisotropy and positive conductive anisotropy, above a certain voltage threshold, the well-known Fréedericksz transition is observed. At a higher value of the applied voltage, it is possible to observe several structures constituted by extremely complex and irregular patterns that are quite different from those observed in a planar sample of the same liquid crystal material. In spite of this, even in this case it is easy to observe the transition between turbulent states. These two turbulent states are optically similar to DSM1 and DSM2 regimes found in the planar case so, for simplicity, we keep the same notation to refer to them.

EXPERIMENTS AND RESULTS

The sample cell consisted of two parallel square ($L \cong 30 \times 30\,\mathrm{mm}^2$) glass plates spaced by two Mylar strips ($d \cong 36\,\mu\mathrm{m}$). The cell surfaces were coated with transparent electrodes of indium tin oxide (ITO) and, in order to obtain homeotropic alignment, were treated by the surfactant *N*,*N*-dimethyl-*N*-[3-(trimethoxysilyl)propyl]-1-octadecanaminium chloride (DMOAP). Then the cells were filled by capillary action with the nematic liquid crystal *N*-(*p*-methoxybenzilidene)-*p*-*n*-butylaniline (MBBA), and mounted in a thermally insulated oven, the temperature of which could be kept at 24 °C by a HAAKE F3 water bath thermostat. Finally, an ac voltage has been applied across the cell (*z* direction). The experimental procedure consisted of two steps: (a) to measure the threshold voltage for the DSM1-DSM2 transition by the experimental setup shown in Fig. 1; and (b) to observe by means of an optical microscope the nucleation of the DSM2 areas, record their growth on videotape, and subsequently to calculate the nucleation rate and the growth velocity from the recorded images.

The experiment was performed at the fixed ac voltage frequency of 70 Hz, but the results do not change qualitatively if the frequency is varied in the conductive regime of the nematic material [10].

In order to check the existence of a threshold voltage for the DSM1-DSM2 transition, V_0 was swept with various rates r (mV/s) in the neighborhood of the DSM1-DSM2 transition. In Fig. 2 the voltage dependence of the light transmittance is shown as a function of both increasing and decreasing applied voltage.

On increasing the voltage, the light transmittance has a sudden change in the slope at the voltage V_J. Above V_J the DSM2 nuclei rise and grow spontaneously and a greater and greater amount of light is scattered out from the transmitted beam (in the homeotropic case we did not observe the strong dependence on the polarization of the incident light which has been found for the planar case). The voltage V_J decreases as r increases; therefore, we can consider it as an

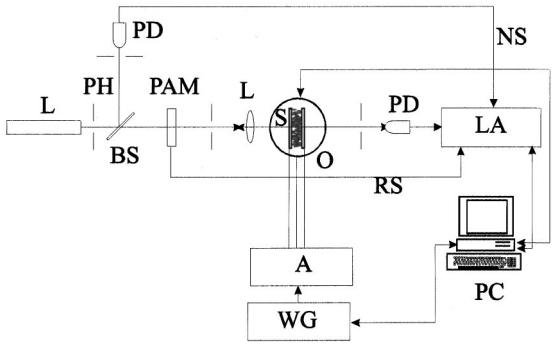

FIG. 1. The experimental setup. *L*, He-Ne laser; PH, pinhole; BS, beam splitter; PD, photodiode; PAM, photoacoustic modulator; *L*, lens; *S*, NLC sample; *O*, oven, *A*, amplifier; WG, wave form generator; LA, lock-in amplifier; PC, personal computer.

*Author to whom correspondence should be addressed.

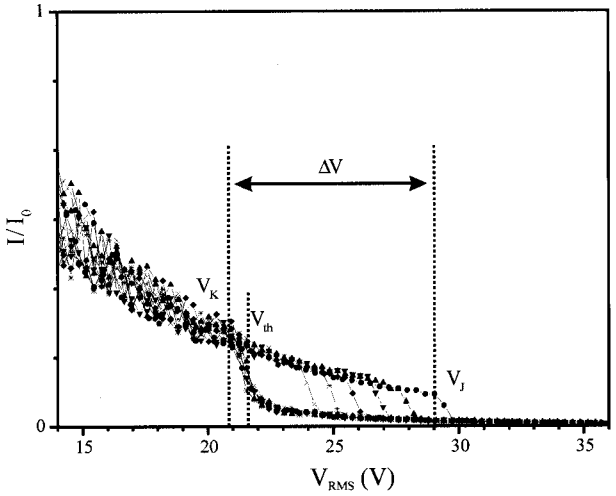

FIG. 2. Hysteresis in the light transmittance I/I_0 near the DSM1-DSM2 transition for various ramp rates r (mV/s). The ramp values used range from 60 to 5 (mV/s) at the fixed frequency of 200 Hz and $T=24\,°\mathrm{C}$.

r-dependent DSM2 threshold. Unlike V_J, the voltage V_k is rather insensitive to changes of r and the difference ΔV between V_J and V_k tends to zero for decreasing r. Because of this behavior we take $V_k=V_{\mathrm{th}}=17.5\,\mathrm{V}$ (at $24\,°\mathrm{C}$) as the DSM2 threshold voltage.

In Fig. 3 there is a series of images which show, at different times, the nucleation phenomenon for both planar and homeotropic samples of NLC. In both cases the temperature was kept at $24\,°\mathrm{C}$ and the external applied voltage was suddenly increased from 0 to ε_2, where $\varepsilon_2=2.1$ (planar) and $\varepsilon_2=10.7$ (homeotropic), where ε_2 is the external control parameter of the transition:

$$\varepsilon_2=\frac{(V_0^2-V_{\mathrm{th}}^2)}{V_{\mathrm{th}}^2}.$$

The darkest regions are the spontaneously created DSM2 nuclei. In time the nuclei grow and merge with other nuclei. Simultaneously new nuclei are created in the remaining DSM1 area until the whole sample is in the DSM2 state.

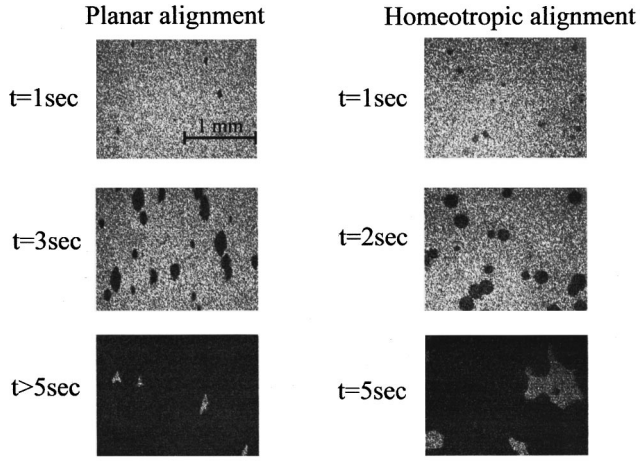

FIG. 3. A set of photographs of the growth process of DSM2 nuclei at different times after applying a voltage V larger than the DSM2 threshold voltage V_{th} (see the text).

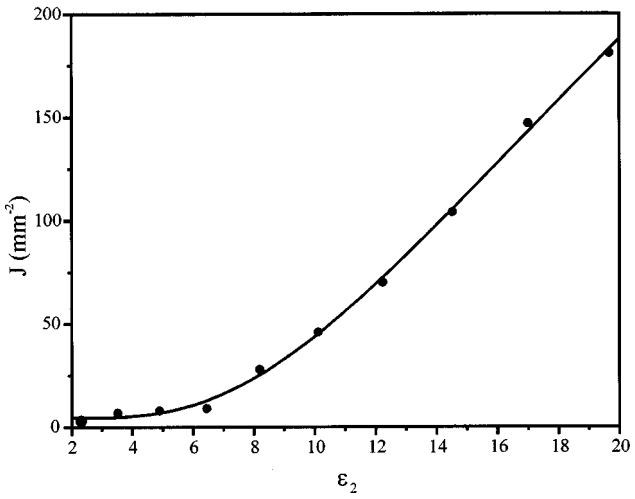

FIG. 4. Nucleation rate J for DSM2 turbulent nuclei as a function of the reduced voltage ε_2.

It is worthwhile to note that in the case of a planarly aligned sample, the DSM2 nuclei are always roughly elliptical in shape with the long axis parallel to the initial planar anchoring direction. On the other hand, in the case of the homeotropically aligned sample, the DSM2 nuclei display a clearly circular form. Moreover, the number of nucleation sites increases and their initial size becomes smaller as the external voltage is increased.

Let us define now the nucleation rate J as the number of DSM2 nuclei spontaneously created, per unit of area, in the time interval ranging from 1 to 2 s after the external control parameter was suddenly increased from 0 to ε_2. In Fig. 4, the nucleation rate J is shown as function of ε_2, at a fixed temperature of $24\,°\mathrm{C}$. The solid line was obtained from the usual expression [12] for the nucleation rates J:

$$J=J_\infty \exp[-A/(1+\varepsilon_2)]+B$$

using the following values for $T=24\,°\mathrm{C}$: $J_\infty=995\,\mathrm{mm}^{-2}$, $A=32$, $B=4.5\,\mathrm{mm}^{-2}$.

Here A corresponds to a normalized potential difference between DSM1 and DSM2 regimes, and B is probably related to the contribution from a heterogeneous nucleation induced by inhomogeneities in the sample and/or on surface electrodes. Using the obtained value of $J_\infty=995\,\mathrm{mm}^{-2}$, it is possible to give information about the minimum area for one nucleation phenomenon [13]. In fact, the obtained value of J_∞ corresponds to a size of about 32 $\mu\mathrm{m}^2$, quite similar to the value of 33 $\mu\mathrm{m}^2$ found in the planar case [13].

On the other hand, in the planar case the value of the temperature-dependent activation energy ($A=50$ for $T=27\,°\mathrm{C}$) [13,14] is greater than the homeotropic one. In other words, the nucleation processes are facilitated, for the same applied voltage, in the homeotropic samples. It is worthwhile to correlate this different activation energy with the difference of the anchoring energy that has been found [15] for homeotropically and planar oriented samples. In fact, the polar (or zenithal) anchoring energy for homeotropically oriented MBBA samples is generally of the order of $10^{-3}-10^{-2}\,\mathrm{erg\,cm}^{-2}$. Instead, for planar oriented samples the polar energy is generally higher ($10^{-2}-1\,\mathrm{erg\,cm}^{-2}$). These remarks seem to be a reasonable confirmation of the

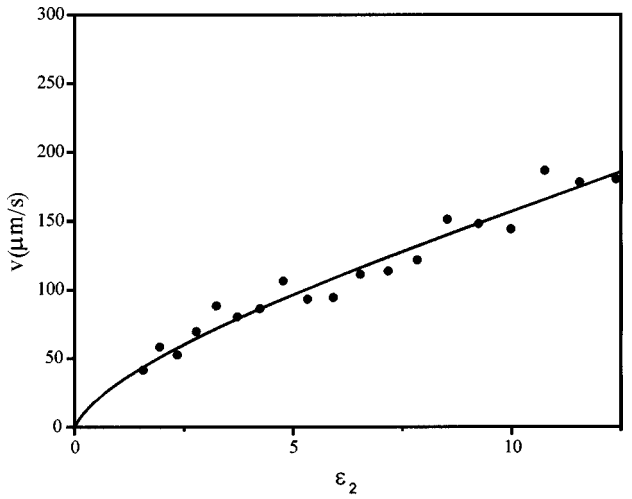

FIG. 5. The growth velocity of the DSM2 turbulent nuclei as a function of the reduced voltage ε_2.

fact that to the basis of the nucleation process there is a breaking of the molecular anchoring at the surface [16–18] that is most easily achieved for the homeotropic orientation.

In Fig. 5 the growth velocity of the DSM2 nuclei as a function of the control parameter ε_2 at $T=24\,^{\circ}\mathrm{C}$ is reported. The solid line represents the expression $\nu=\gamma\varepsilon_2^{0.7}$, where $\gamma=32\,\mu$m/s at 24 °C has been chosen for the best fit. Similar values of γ were obtained for planar samples of NLC, although in the planar case two different nucleus growth velocities exist, one parallel, the other perpendicular to the original undistorted director orientation [13,17].

Unfortunately, problems related to the low optical contrast values hinder us in measuring the growth velocity for values of $\varepsilon_2<1.5$.

CONCLUSIONS

In this work the electrohydrodynamic pattern forming instability driven by an ac voltage applied to a homeotropically oriented nematic liquid crystal layer has been experimentally studied near onset.

It is worthwhile to draw a parallel between the homeotropic and the planar cases. The DSM1→DSM2 transition both in planar and homeotropic samples is a threshold phenomenon, although in the latter case the threshold voltage is much lower.

Contrary to the planar, where the DSM2 nuclei are always roughly elliptical in shape with the long axis parallel to the original undistorted director orientation, in the homeotropic sample, the DSM2 nuclei have a circular form.

We are able to give some quantitative information about important parameters governing the nucleation phenomenon in the turbulent-turbulent transition. Both the nucleation rate and the growth speed of the nucleated DSM2 areas are about the same for homeotropic and planar samples. For the same external applied voltage, we have found also the same minimum area for one nucleation phenomenon. In contrast, the activation energy and the ac voltage threshold are lower for the homeotropic orientation. Our measurements confirm that the nucleation process is facilitated for the homeotropic orientation and suggest that the transition would be a surface phenomenon in which the anchoring strength is mainly involved. Once the anchoring is broken, the dynamics of the nucleation process is the same for both the planar and the homeotropic orientation.

In conclusion we think that a better understanding of electrohydrodynamics and, in particular, of the nucleation phenomenon that takes place at the DSM1→DSM2 transition, could be useful to gain insight into the problem of the anchoring breakage, which is of interest for the novel LCD technology.

ACKNOWLEDGMENTS

The authors are indebted to R. Bartolino for a fruitful discussion and for helpful suggestions. The authors would like to thank B. De Nardo and C. Prete for their technical aid.

[1] R. P. Behringer, Rev. Mod. Phys. **57**, 657 (1985); S. Kai, M. Andoh, and S. Yamaguchi, Phys. Rev. A **46**, 375 (1992).
[2] J. T. Tough, in *Superfluid Turbulence in Low Temperature Physics*, edited by D. F. Brewer (North-Holland, Amsterdam, 1982).
[3] A. Sussma, Appl. Phys. Lett. **21**, 269 (1972).
[4] S. Kai, K. Hayashi, and Y. Hidaka, J. Phys. Chem. **100**, 19 016 (1996).
[5] Y. Hidaka, J. Huh, K. Hayashi, S. Kai, and M. I. Tribelsky, Phys. Rev. E **56**, R6256 (1997).
[6] H. Richter, N. Klopper, A. Hertrich, and A. Buka, Europhys. Lett. **30**, 37 (1995).
[7] H. Richter, A. Buka, and I. Rehberg, Phys. Rev. E **51**, 5886 (1995).
[8] A. G. Rossberg, A. Hertrich, L. Kramer, and W. Pesh, Phys. Rev. Lett. **76**, 4729 (1996).
[9] A. Hertrich, W. Decker, W. Pesh, and L. Kramer, J. Phys. II **2**, 1930 (1992).
[10] P. G. de Gennes and J. Prost, *The Physics of Liquid Crystals* (Oxford University Press, New York, 1993).
[11] M. I. Tribelsky and K. Tsuboi, Phys. Rev. Lett. **76**, 1631 (1996).
[12] F. F. Abraham, *Homogeneous Nucleation Theory* (Academic, New York, 1974).
[13] S. Kai and W. Zimmermann, Prog. Theor. Phys. Suppl. **99**, 458 (1989).
[14] S. Kai, W. Zimmermann, M. Andoh, and N. Chizumi, Phys. Rev. Lett. **64**, 1111 (1990).
[15] L. M. Blinov and V. G. Chigrinov, *Electrooptic Effects in Liquid Crystal Materials* (Springer-Verlag, Berlin, 1994).
[16] V. Carbone, N. Scaramuzza, and C. Versace, Physica D **106**, 314 (1997).
[17] N. Scaramuzza, C. Versace, and V. Carbone, Mol. Cryst. Liq. Cryst. Sci. Technol., Sect. A **266**, 85 (1995).
[18] V. S. U. Fazio and L. Komitov, Europhys. Lett. **46**, 38 (1999).